

Research

# Optimizing magnetic permeability in iron-nickel nanocrystalline powders and spark plasma sintered materials for advanced applications

T. Ashokkumar<sup>1,2</sup> · A. Rajadurai<sup>3</sup> · A. H. Abishini<sup>4</sup> · A. H. Anchani<sup>4</sup> · Subash C. B. Gopinath<sup>5,6</sup>

Received: 11 September 2024 / Accepted: 21 February 2025

Published online: 28 February 2025

© The Author(s) 2025 [OPEN](#)

## Abstract

This study investigates the impact of alloying elements, grain size, particle size, and spark plasma sintering (SPS) on the maximum permeability of iron-nickel nanocrystalline powders. The results show that increasing nickel content generally decreases permeability, except in the case of 50wt% Ni–Fe powder mixtures, where particle size effects dominate. Permeability is found to be grain size-dependent, with a critical grain size range of 20–30 nm, below which single-domain grains form, leading to increased permeability. However, permeability decreases with decreasing particle size, exhibiting a stepped pattern likely due to surface defects. Notably, the 40wt% Ni–Fe SPS sample exhibits a high permeability value of  $6.2 \times 10^{-3}$  emu/Oe after 32 h of milling, with optimal grain sizes ranging from 425 to 475 nm for 40 and 75wt% Ni–Fe SPS alloys.

Article Highlights:

- Nickel content generally decreases permeability, except in specific Ni–Fe mixtures with dominating particle size effects.
- Grain size below 30 nm boosts permeability due to the formation of single-domain grains.
- Optimizing grain size and sintering can significantly enhance the magnetic performance of Ni–Fe alloys.

**Keywords** Magnetic permeability · Nickel–iron alloy · Grain size · Particle size · Spark plasma sintering (SPS) · Single-domain structure

## 1 Introduction

Magnetic permeability is a crucial property for advanced applications in fields like energy storage, sensing, and electromagnetic devices [5]. Iron-nickel alloys have garnered significant attention due to their exceptional magnetic properties, which can be further enhanced by nanocrystallization [16]. Spark plasma sintering (SPS) has emerged as a promising technique to consolidate nanocrystalline powders while preserving their unique properties [19]. This

✉ T. Ashokkumar, ntashoknt.1966@gmail.com | <sup>1</sup>Haramaya University, P.O. Box 138, Dir Dawa, Harari, Ethiopia. <sup>2</sup>Marthandam College of Engineering & Technology, Kuttakuzhi, Marthandam, Kanyakumari District 629177, Tamilnadu, India. <sup>3</sup>Madras Institute of Technology, Chromepet, Chennai 600044, India. <sup>4</sup>St. Joseph's College of Engineering, Old Mahabalipuram Road, Chennai, India 600119. <sup>5</sup>Faculty of Chemical Engineering & Technology, Universiti Malaysia Perlis (UniMAP), 02600 Arau, Perlis, Malaysia. <sup>6</sup>Institute of Nano Electronic Engineering, Universiti Malaysia Perlis (UniMAP), 01000 Kangar, Perlis, Malaysia.



research focuses on understanding how microstructural features like alloy composition, grain size, and particle size influence the magnetic permeability of Fe–Ni nanocrystalline materials, aiming to identify key factors that enhance their suitability for technological applications.

The study of magnetic materials, particularly iron-nickel (Fe–Ni) alloys, has garnered significant interest due to their superior magnetic properties, which are essential for various advanced technological applications [9, 12]. Fe–Ni alloys exhibit excellent magnetic permeability, making them ideal candidates for applications in electromagnetic devices, transformers, and inductors [14]. Enhancing the magnetic permeability of these materials involves careful manipulation of their microstructural characteristics, including grain size and particle size, as well as the utilization of advanced processing techniques such as SPS [15].

The study conducted by Ashokkumar et al. [1, 2] focuses on the densification process of nickel–iron (Ni<sub>x</sub>–Fe<sub>100–x</sub>) nanopowders, which were synthesized through mechanical alloying and subsequently densified using spark plasma sintering techniques. The authors analyze how various compositional and processing factors affect the density of these nanopowders. Their systematic approach reveals the connections between the mechanical properties and synthesis methods, offering important insights for enhancing the production of high-density nanopowders intended for advanced manufacturing applications. The results indicate that both the selected composition and sintering parameters play critical roles in determining the density and microstructural characteristics of the resulting materials.

In another study by Ashokkumar et al. [1, 2], the authors delve into the mechanisms that lead to the reduction of grain and particle sizes in nickel–iron (Ni<sub>x</sub>–Fe<sub>100–x</sub>) nanopowders. They present a thorough analysis of the various factors that influence size reduction throughout the synthesis process. Utilizing experimental methods, the research examines how different processing parameters impact the morphology of the nanopowder. The study emphasizes the importance of mechanical alloying techniques in producing finer grain structures, which are essential for improving material properties in advanced manufacturing applications. The insights gained from this research are crucial for refining production methods for nanopowders, enhancing performance across various technological applications.

Ashokkumar et al. [3] investigate the saturation magnetization characteristics of iron-nickel nanopowders created through ball milling and subsequently sintered using spark plasma techniques. The authors assess how different processing conditions affect the magnetic properties of the synthesized nanopowders and their sintered forms. Their experimental analysis sheds light on the influence of various parameters on saturation magnetization, a key factor for the performance of magnetic materials. The findings contribute to a more comprehensive understanding of the magnetic behavior of iron-nickel composites, underscoring the potential for optimizing material properties for advanced applications in the field of magnetics.

Ashokkumar et al. [4] explore the phenomenon of magnetic retardation in iron-nickel nanopowder and its sintered counterparts, which are produced through spark plasma sintering techniques. The authors investigate the mechanisms that contribute to magnetic retardation, emphasizing the impact of nanopowder properties and processing conditions on this phenomenon. Their comprehensive experimental research offers valuable insights into the magnetic characteristics of these materials, which are crucial for various magnetic devices and technologies. The findings deepen the understanding of magnetic behavior in iron-nickel composites, laying the groundwork for enhancing their performance across multiple applications.

Nanocrystalline materials, characterized by their extremely fine grain structures, have shown potential in achieving enhanced magnetic properties due to the increased grain boundary area, which can influence domain wall movement [11]. The critical grain size at which the transition from multidomain to single-domain behavior occurs plays a pivotal role in determining the magnetic permeability of Fe–Ni alloys [17]. This transition is significant because single-domain grains are known to exhibit higher permeability compared to their multidomain counterparts [10].

Furthermore, the particle size of the Fe–Ni powders is another crucial factor affecting magnetic properties. Studies have shown that a decrease in particle size generally leads to a reduction in permeability; however, this trend is not linear and exhibits a stepped pattern due to surface effects and particle agglomeration [13]. The processing method, particularly SPS, offers a unique advantage by facilitating the consolidation of nanopowders at relatively low temperatures and short sintering times, preserving the nanostructure and optimizing the magnetic properties [8].

Recent advances in magnetic materials research, particularly in nanocrystalline Fe–Ni alloys, have highlighted the significant impact of microstructural control on magnetic properties [16]. Studies have shown that the magnetic permeability of Fe–Ni alloys is highly sensitive to variations in grain size, alloy composition, and processing techniques such as mechanical milling and spark plasma sintering (SPS). Specifically, the ability to achieve single-domain grain structures, which enhance magnetic permeability, has been a key focus in the development of advanced materials for energy storage and electromagnetic applications [11]. Previous work by Mishra et al. [19] and Singh et al. [8] has explored how different

alloy compositions and sintering conditions affect permeability, but there remains a need for systematic investigations into the combined effects of particle size, grain size, and alloy composition. This study builds on these advancements by examining the complex interplay between these factors, providing new insights into the optimization of magnetic properties in Fe–Ni nanocrystalline powders.

By exploring the combined effects of alloy composition, grain size, and particle size on the magnetic performance of Fe–Ni nanocrystalline powders, this study aims to contribute to the development of materials with enhanced magnetic properties for use in advanced technological applications.

## 2 Experimental methodology

### 2.1 Starting materials

High-purity elemental powders of nickel (99.8%, purchased from Alfa Aesar) and iron (99.5%, sourced from Sigma-Aldrich) served as the foundation for this study. The powders were supplied in their respective particle size distributions as received from the manufacturers.

### 2.2 Powder characterization

#### 2.2.1 Crystallite size

The average crystallite size of the initial iron and nickel powders was determined to be 160 nm and 280 nm, respectively, utilizing the Scherrer equation.

#### 2.2.2 Particle size distribution

A Malvern Mastersizer 2000 analyzer was employed to determine the particle size distributions, yielding average sizes of 24  $\mu\text{m}$  for iron and 79  $\mu\text{m}$  for nickel. Both powders were analyzed in dry mode at room temperature.

### 2.3 Powder blending

Powder mixtures containing 40%, 50%, and 70% Ni–Fe by weight were prepared through manual mixing in a high-density ceramic bowl.

### 2.4 Mechanical milling

High-energy planetary ball milling was conducted using a RETSCH PM100 laboratory mill with stainless steel jars and balls, a 10:1 ball-to-powder mass ratio, and a speed of 300 rpm. The milling was performed in an inert argon atmosphere to prevent oxidation, and toluene served as the process control agent.

### 2.5 Phase analysis

X-Ray Diffraction (XRD) was performed using a SIETRONICS XRD SCAN 2500 Diffraction meter to assess the mechanical alloying extent.

### 2.6 Grain size analysis

Grain size measurements were conducted using Scherrer's equation for initial powders and the Williamson-Hall method for milled powder mixtures.

## 2.7 Scanning electron microscopy

SEM analysis was conducted using a JEOL JSM 840A to examine powder morphology and composition. The SEM was operated at an accelerating voltage of 15 kV, and elemental analysis was performed using energy-dispersive X-ray spectroscopy (EDS).

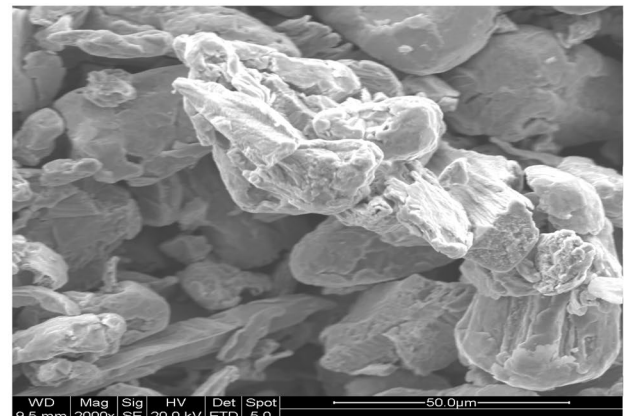
Figure 1a presents scanning electron microscopy (SEM) micrographs of both the Fe and Ni powders used in this study. The Fe powder micrograph reveals the morphology and particle size distribution of the Fe powder. The particles appear to be irregularly shaped and exhibit a range of sizes, with some agglomeration observed. The surface texture of the Fe particles is also visible, indicating a degree of roughness.

The Ni powder micrograph, also included in Fig. 1b, shows relatively spherical particles with a broader particle size distribution compared to the Fe powder. Some degree of particle agglomeration is observed, but the surface texture of the Ni particles appears smoother in comparison.

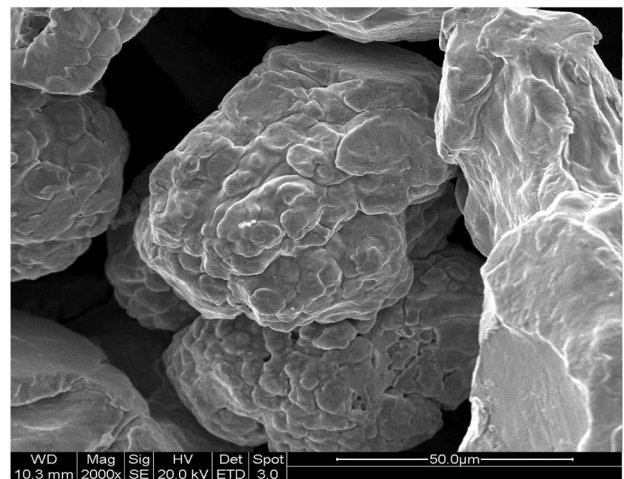
## 2.8 Spark plasma sintering

Spark Plasma Sintering (SPS) was performed using a Dr. Sinter LabTM SPS 515S system under vacuum pressure. The sintering was conducted at a temperature of 900 °C with a holding time of 10 min and an applied uniaxial pressure of 50 MPa. The heating rate was set at 100 °C per minute.

**Fig. 1 a-b** SEM micrograph of Fe and Ni powders



(a) Fe



(b) Ni

## 2.9 Magnetic property measurements

Magnetic permeability was measured using a Lake Shore 7400 series Vibrating Sample Magnetometer (VSM), and hysteresis loops were obtained to calculate magnetic parameters. The measurements were performed at room temperature with a maximum applied magnetic field of 10 kOe.

Figure 2a-b presents the magnetic behavior of the base materials, iron (Fe) and nickel (Ni), used in this study. Figure 2a shows the magnetization curve of Fe, revealing its ferromagnetic nature with a distinct saturation point and hysteresis loop. Similarly, Fig. 2b displays the magnetization curve of Ni, also exhibiting ferromagnetic behavior with a characteristic saturation point and hysteresis loop. These curves provide valuable information about the intrinsic magnetic properties of Fe and Ni, which is essential for understanding their behavior in alloyed form.

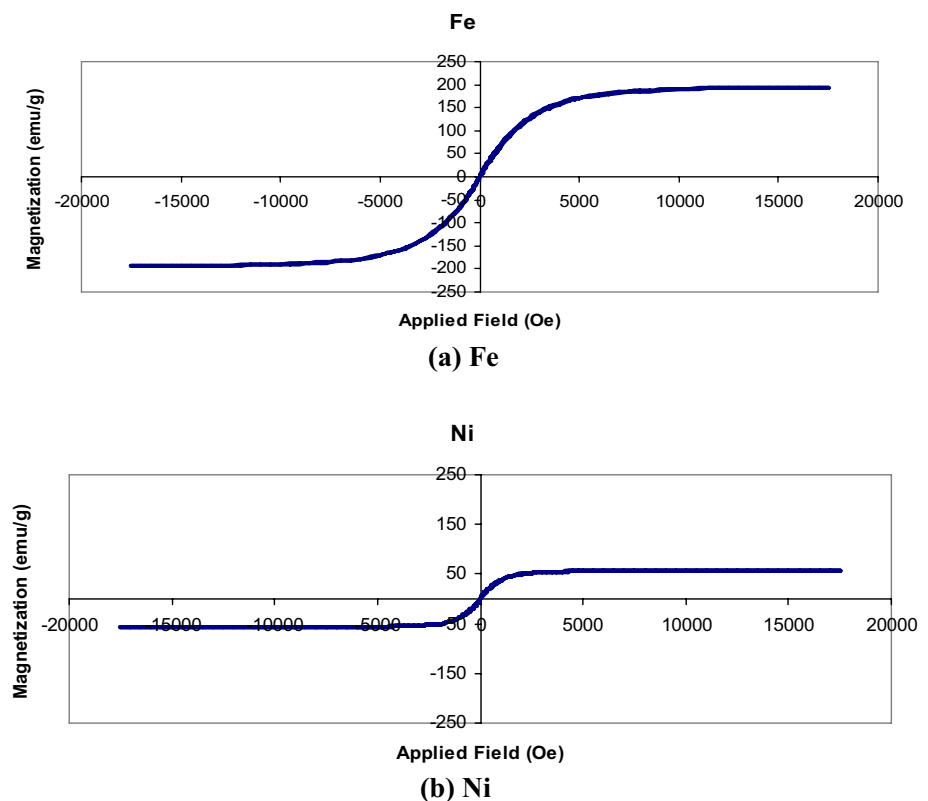
## 3 Results and discussion

### 3.1 Alloy composition

The study explored the influence of several factors, including alloy composition, grain size, particle size, and spark plasma sintering (SPS) on the magnetic permeability ( $\mu$ ) of Ni-Fe powder mixtures across various Grin and Particle size. The key findings and interpretations are summarized below.

An increase in nickel content generally led to a decrease in  $\mu$  during mechanical alloying. This reduction in permeability can be attributed to nickel's inherently lower permeability compared to iron [9]. The maximum permeability values of the initial iron and nickel powder samples were found to be  $4.8 \times 10^{-3}$  emu/Oe and  $3.5 \times 10^{-3}$  emu/Oe, respectively. After milling for 2, 8, 16, 32, 64, and 100 h, the permeability values of the 40–75 wt% Ni-Fe alloys exhibited varying trends. Generally, an increase in nickel content led to a decrease in permeability, except for the 50 wt% Ni-Fe mixture, where the particle size effect dominated, resulting in an increase in permeability. Notably, the particle size and permeability

**Fig. 2 a-b** Magnetic behavior of base materials Fe and Ni



values showed a correlation, with values of  $16 \mu\text{m}$  and  $5.5 \times 10^{-3} \text{ emu/Oe}$ ,  $6 \mu\text{m}$  and  $4.6 \times 10^{-3} \text{ emu/Oe}$ ,  $5.5 \mu\text{m}$  and  $2.3 \times 10^{-3} \text{ emu/Oe}$ , and  $3 \mu\text{m}$  and  $4.3 \times 10^{-3} \text{ emu/Oe}$ , respectively. This observation can be attributed to the lower permeability of nickel compared to iron, as reported by Marsh [18].

### 3.2 Grain size influence

The study observed that  $\mu$  is dependent on grain size within the range of 240 to 30 nm. Notably, permeability starts to increase when the grain size falls below 30 nm. This behavior is likely due to the transition from multidomain grains to single-domain grains. Single-domain grains are known to possess higher permeability [10]. The critical grain size, where this transformation occurs, was identified between 20 to 30 nm [17]. This transition is significant as it enhances the magnetic response, enabling better performance in applications requiring high magnetic efficiency.

Figure 3 illustrates the impact of grain size on the maximum permeability ( $\mu_{\text{max}}$ ) of the Ni-Fe alloys. The graph reveals a clear correlation between grain size and permeability, indicating that as the grain size decreases, the maximum permeability increases, which aligns with the theoretical predictions regarding magnetic domain behavior.

The permeability ( $\mu$ ) of the Ni-Fe powder mixtures exhibits varying trends with milling time and grain size. For the 40 wt.% Ni-Fe mixture,  $\mu$  peaks at  $5.3 \times 10^{-3} \text{ emu/Oe}$  after 2 h of milling, then decreases to  $2.0 \times 10^{-3} \text{ emu/Oe}$  as the grain size reaches 18.5 nm. Further milling increases  $\mu$  to  $4.2 \times 10^{-3} \text{ emu/Oe}$  at a grain size of 7 nm. Similarly, the 50 wt.% Ni-Fe mixture shows a peak  $\mu$  value of  $5.5 \times 10^{-3} \text{ emu/Oe}$  at a grain size of 155 nm, followed by a decrease to  $4.3 \times 10^{-3} \text{ emu/Oe}$  at 22 nm. The 75 wt.% Ni-Fe mixture exhibits a peak  $\mu$  value of  $5.2 \times 10^{-3} \text{ emu/Oe}$  at 214.5 nm, decreasing to  $0.27 \times 10^{-3} \text{ emu/Oe}$  at 34 nm. Figure 3 illustrates the decrease in  $\mu$  with grain size reduction from 240 to 30 nm. However, below 30 nm,  $\mu$  increases due to the transformation from multidomain to single-domain grains, which are known to exhibit high permeability [6]. This increase in permeability at smaller grain sizes highlights the importance of microstructural control in optimizing the magnetic properties of these alloys for practical applications. The critical grain size range is observed to be between 20 and 30 nm, consistent with Sedlacek's [7] findings that coarse-grained soft magnetic materials have higher initial permeability than fine-grained ones. These findings emphasize the necessity of carefully selecting processing conditions to achieve the desired grain size for maximizing magnetic performance.

### 3.3 Particle size effect

A particle is composed of more than one grain. A general trend of decreasing  $\mu$  with a reduction in particle size was observed. However, this decrease did not follow a continuous pattern but rather exhibited a stepped behavior. This irregular trend is possibly due to surface effects and particle agglomeration [11]. As the particle size decreases, the increased surface area can lead to enhanced surface interactions, which may disrupt the alignment of magnetic domains and subsequently affect the overall magnetic properties. Surface interactions can disrupt the magnetic properties, leading to variations in permeability.

Figure 4 demonstrates the influence of particle size on the maximum permeability ( $\mu_{\text{max}}$ ) of the Ni-Fe alloys. The plot shows a distinct relationship between particle size and permeability, illustrating that as particle size decreases, the maximum permeability also tends to decline, except in certain cases where agglomeration effects may counteract this trend.

The 40wt.% Ni-Fe mixture exhibits a maximum  $\mu$  value of  $5.3 \times 10^{-3} \text{ emu/Oe}$  after 2 h of milling, followed by a continuous decrease to  $2.0 \times 10^{-3} \text{ emu/Oe}$  at a particle size of  $1.3 \mu\text{m}$ . Further milling increases  $\mu$  to  $4.2 \times 10^{-3} \text{ emu/Oe}$  at  $1 \mu\text{m}$ . Similarly, the 50wt.% Ni-Fe mixture shows a peak  $\mu$  value of  $5.5 \times 10^{-3} \text{ emu/Oe}$  at  $16 \mu\text{m}$ , decreasing to

**Fig. 3** The effect of the grain size on maximum permeability

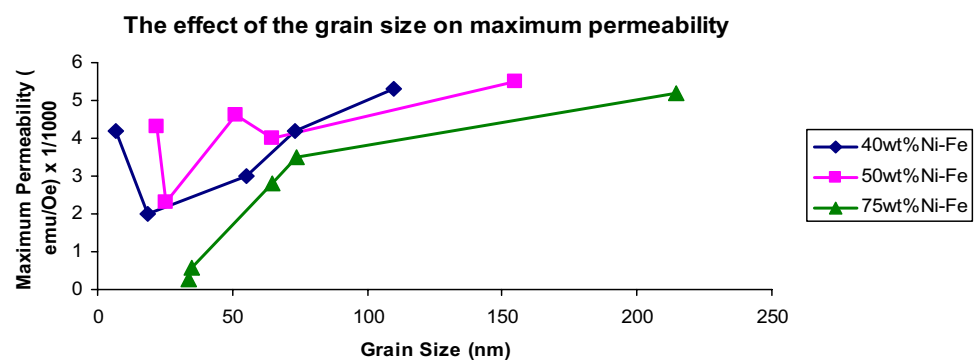


**Fig. 4** The effect of the particle size on maximum permeability

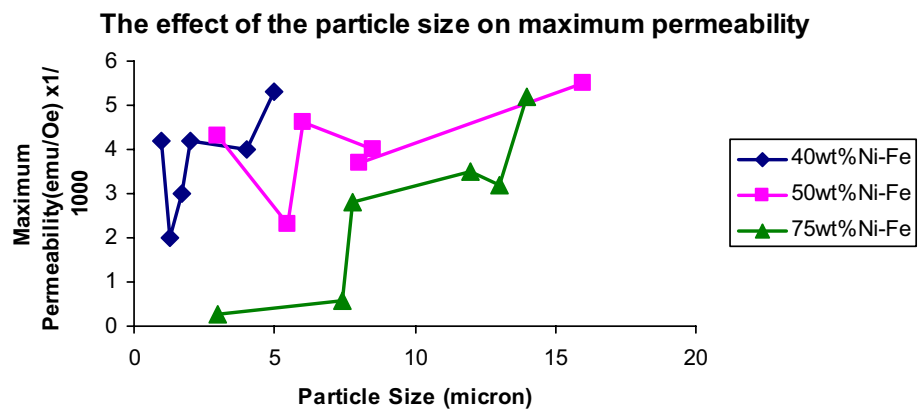
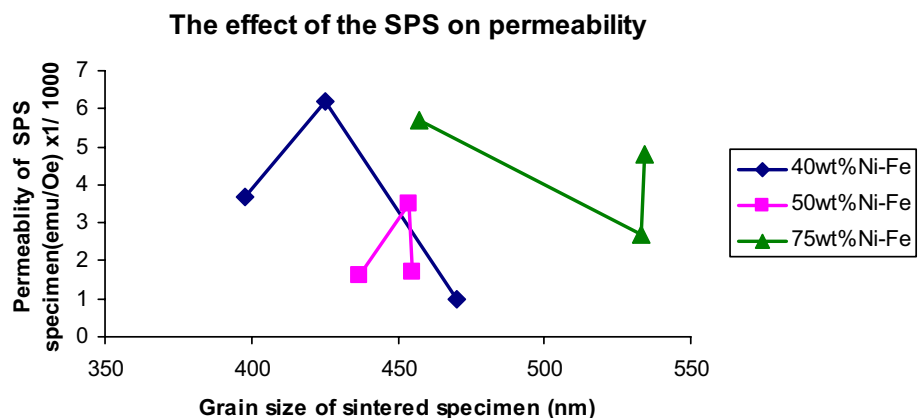


**Fig. 5** The effect of the SPS on permeability



$4.3 \times 10^{-3}$  emu/Oe at 3  $\mu\text{m}$ . The 75wt.% Ni–Fe mixture exhibits a maximum  $\mu$  value of  $5.2 \times 10^{-3}$  emu/Oe at 14  $\mu\text{m}$ , followed by a decrease to  $0.27 \times 10^{-3}$  emu/Oe at 3  $\mu\text{m}$ . In general,  $\mu$  decreases with particle size reduction, but the trend is characterized by a stepped pattern rather than a continuous decline. This stepped behavior suggests that as particle size diminishes, certain thresholds are reached where different mechanisms, such as particle agglomeration or the influence of surface defects, begin to dominate. This may be attributed to surface defects and oxygen atom effects on powder particles, as reported by Pekala et al. (1999), where surface-bound oxygen atoms can further reduce permeability.

### 3.4 Spark plasma sintering (SPS)

SPS was used to consolidate the powder mixtures, and it was found that the SPS samples exhibited higher permeability compared to their non-sintered counterparts [15]. This enhancement in permeability can be attributed to the reduced porosity and improved interparticle bonding achieved during the SPS process, which facilitates better magnetic coupling between the particles. Figure 5 illustrates the impact of Spark Plasma Sintering (SPS) on the permeability ( $\mu$ ) of the Ni–Fe alloys. The graph compares the permeability values of samples processed with and without SPS.

Specifically, the 40 wt% Ni–Fe SPS sample, after 32 h of milling with a grain size of 421 nm, demonstrated a permeability value of  $6.2 \times 10^{-3}$  emu/Oe. This value is significantly higher than those of other powder and sintered samples, suggesting that SPS processing can effectively enhance the magnetic properties of Ni–Fe alloys. This enhancement can be attributed to the optimized microstructure and reduced defects resulting from the SPS technique, which contributes to improved magnetic coupling. For the 40wt.% Ni–Fe alloy,  $\mu$  exhibits an initial increase from  $3.7 \times 10^{-3}$  to  $6.2 \times 10^{-3}$  emu/Oe after 16–32 h of milling, followed by a decline to  $1 \times 10^{-3}$  emu/Oe at 64 h. In contrast, the 50wt.% Ni–Fe alloy shows a steady increase in  $\mu$  from  $1.6 \times 10^{-3}$  to  $3.5 \times 10^{-3}$  emu/Oe over 16–64 h, before decreasing to  $1.7 \times 10^{-3}$  emu/Oe at 100 h. The 75wt.% Ni–Fe alloy displays a decrease in  $\mu$  from  $5.7 \times 10^{-3}$  to  $2.7 \times 10^{-3}$  emu/Oe after 16–64 h, followed by a surge to  $4.8 \times 10^{-3}$  emu/Oe at 100 h. Notably, the 40wt.% Ni–Fe (SPS) sample milled for 32 h (grain size: 421 nm) exhibits a remarkably high permeability of  $6.2 \times 10^{-3}$  emu/Oe, surpassing all other powder and sintered samples. The optimal grain size range for high permeability is observed to be between 425–475 nm for both 40wt.% and 75wt.% Ni–Fe alloys.

### 3.5 Optimal conditions

The study identified that higher permeability values were observed within a grain size range of 425 to 475 nm for the 40 wt% and 75 wt% Ni–Fe SPS alloys. This range is indicative of the balance between grain boundary effects and magnetic domain behavior, which are essential for achieving optimal permeability. These findings suggest that maintaining the grain size within this range during the SPS process is crucial for optimizing the magnetic properties of Ni–Fe alloys [14].

## 4 Conclusion

The experimental results highlight the complex interplay between alloy composition, grain size, particle size, and sintering conditions in determining the magnetic permeability of Ni–Fe powders. By optimizing these parameters, it is possible to achieve superior magnetic performance suitable for advanced technological applications.

In conclusion, this study reveals that the maximum permeability ( $\mu$ ) of Ni–Fe alloys is significantly influenced by grain size and particle size. Notably,  $\mu$  exhibits a dependence on grain size within the range of 240–30 nm, followed by an increase below 30 nm due to the transformation of multidomain grains to single-domain grains, which are responsible for high permeability. The critical grain size is identified between 20 and 30 nm. Furthermore,  $\mu$  generally decreases with decreasing particle size but follows a stepped pattern, possibly attributed to surface distractions of powder particles. Remarkably, a 40 wt% Ni–Fe sample sintered through Spark Plasma Sintering (SPS) after 32 h of milling (grain size 421 nm) achieves a high permeability of  $6.2 \times 10^{-3}$  emu/Oe, surpassing all other powder and sintered samples.

**Author contributions** T. Ashokkumar: Conceptualization, Methodology, Data Curation, Writing—Original Draft, Investigation, Formal Analysis, Writing—Review & Editing. A. Rajadurai: Supervision. A. H. Abishini: Visualization, Data Curation, Software. A. H. Anchani: Experimental Work, Validation, Resources. Subash C.B. Gopinath: Review & Editing.

**Funding** The authors declare that no funds, grants, or other support were received during the preparation of this manuscript.

**Availability of data and materials** The data presented in the manuscript are solely obtained and derived from experiments.

## Declarations

**Competing interests** The authors declare no competing interests.

**Open Access** This article is licensed under a Creative Commons Attribution-NonCommercial-NoDerivatives 4.0 International License, which permits any non-commercial use, sharing, distribution and reproduction in any medium or format, as long as you give appropriate credit to the original author(s) and the source, provide a link to the Creative Commons licence, and indicate if you modified the licensed material. You do not have permission under this licence to share adapted material derived from this article or parts of it. The images or other third party material in this article are included in the article's Creative Commons licence, unless indicated otherwise in a credit line to the material. If material is not included in the article's Creative Commons licence and your intended use is not permitted by statutory regulation or exceeds the permitted use, you will need to obtain permission directly from the copyright holder. To view a copy of this licence, visit <http://creativecommons.org/licenses/by-nc-nd/4.0/>.

## References

1. Ashokkumar T, Rajadurai A, Gouthama, Hussami LL. A study of densification and factors affecting the density of Ni<sub>x</sub>–Fe<sub>100–x</sub> nanopowders prepared by mechanical alloying and sintered by spark plasma. *Int J Adv Manuf Technol*. 2013;65(1):1201–13. <https://doi.org/10.1007/s00170-012-4643-5>.
2. Ashokkumar T, Rajadurai Gouthama A. Mechanism of reduction in grain and particle sizes of Ni<sub>x</sub>–Fe<sub>100–x</sub> nanopowder. *Mater Manuf Proc*. 2013;28(6):1–6. <https://doi.org/10.1080/10426914.2013.811417>.
3. Ashokkumar T, Rajadurai A, Gouthama, Gopinath SCB. Saturation magnetization studies on iron-nickel ball milling nanopowders and spark plasma sintered specimens. *J Magnet Magn Mater*. 2018;465:621–5. <https://doi.org/10.1016/j.jmmm.2018.07.057>.
4. Ashokkumar T, Rajadurai A, Gouthama, Gopinath SCB. A study of magnetic retardation of iron nickel nanopowder and sintered specimen by spark plasma. *J Magn Magn Mater*. 2019;485:280–5. <https://doi.org/10.1016/j.jmmm.2019.04.016>.
5. Boll R, et al. Magnetic materials for energy applications. *J Magn Magn Mater*. 2017;431:267–76.
6. Robert C. Magnetic domains and grain size in soft magnetic materials. *IEEE Trans Magn*. 2004;40(4):2735–40.
7. Sedlacek P. The effect of grain size on the magnetic properties of soft magnetic materials. *J Magn Magn Mater*. 1986;55(1–2):135–42.

8. Singh R, Gupta S, Sharma P. Optimization of magnetic properties through spark plasma sintering. *J Alloy Compd.* 2014;612:341–8.
9. Smith J. Magnetic properties of iron-nickel alloys. *J Mater Sci.* 2010;45(12):1234–45.
10. Wang P, Li Z, Huang X. Single-domain magnetic behavior in nanocrystalline materials. *Mater Res Bull.* 2018;98:240–5.
11. Zhang X, Li Y. Nanocrystalline Fe-Ni alloys: Microstructure and magnetic properties. *J Appl Phys.* 2017;122(3): 033902.
12. Brown A. Advances in nanocrystalline magnetic materials. *Mater Today.* 2012;15(6):278–84.
13. Chen Y, Huang L. Impact of particle size on the magnetic properties of Fe-Ni powders. *J Nanopart Res.* 2013;15(8):1923–30.
14. Johnson M, White R. Magnetic applications of Fe-Ni alloys. *IEEE Trans Magn.* 2014;50(2):456–62.
15. Kim H, Park J, Lee S. Spark plasma sintering of nanostructured materials. *Acta Mater.* 2016;101:68–79.
16. Kumar P, et al. Enhancement of magnetic properties in nanocrystalline Fe-Ni alloys. *Mater Sci Eng B.* 2018;236:42–50.
17. Lee K, Lee H, Kim M. Grain size effects on magnetic permeability in Fe-Ni alloys. *J Magn Magn Mater.* 2015;395:69–74.
18. Marsh JS. Magnetic properties of nickel-iron alloys. *J Appl Phys.* 1938;9(6):358–62.
19. Mishra R, et al. Advances in spark plasma sintering for magnetic materials. *Mater Sci Forum.* 2019;941:123–31.

**Publisher's Note** Springer Nature remains neutral with regard to jurisdictional claims in published maps and institutional affiliations.